Phase behavior and structure formation of hairy-rod supramolecules

Subbotin, A; Stepanyan, R; Knaapila, M; Ikkala, O; ten Brinke, G

Published in:
European Physical Journal E

DOI:
10.1140/epje/i2003-10065-y

Publication date:
2003

Eur. Phys. J. E **12**, 333–345 (2003)
DOI 10.1140/epje/i2003-10065-y

THE EUROPEAN PHYSICAL JOURNAL E

Phase behavior and structure formation of hairy-rod supramolecules

A. Subbotin[1,2], R. Stepanyan[1], M. Knaapila[3], O. Ikkala[3], and G. ten Brinke[1,3,a]

[1] Department of Polymer Science and Material Science Center, University of Groningen, Nijenborgh 4, 9747 AG Groningen, The Netherlands
[2] Institute of Petrochemical Synthesis, Russian Academy of Sciences, Moscow 119991, Russia
[3] Department of Engineering Physics and Mathematics, Helsinki University of Technology, P.O. Box 2200, FIN-02015 HUT, Espoo, Finland

Received 21 March 2003 and Received in final form 10 June 2003 /
Published online: 21 November 2003 –

Abstract. Phase behavior and microstructure formation of rod and coil molecules, which can associate to form hairy-rod polymeric supramolecules, are addressed theoretically. Association induces considerable compatibility enhancement between the rod and coil molecules and various microscopically ordered structures can appear in the compatibility region. The equilibria between microphase-separated states, the coil-rich isotropic liquid and the rod-rich nematic are discussed in detail. In the regime where hairy-rod supramolecules with a high grafting density appear as a result of the association, three phase diagram types are possible depending on the value of the association energy. In the low grafting density regime only the lamellar microstructure is proven to be stable.

PACS. 36.20.-r Macromolecules and polymer molecules – 64.60.Cn Order-disorder transformations; statistical mechanics of model systems

1 Introduction

Hairy-rod polymers [1–3] consist of a stiff macromolecular backbone with a large number of flexible side chains. Due to these side chains hairy-rod polymers often exhibit sufficient solubility in common organic solvents and exhibit melting points below temperatures where thermal decomposition prevails [1,2]. This allows melt and solution processibility of otherwise nearly intractable rigid-rod polymers. They received a lot of attention, in particular in the context of electrical conductivity (see Ref. [4] and references therein) since there the backbones consist of conjugated rigid polymers.

As other block copolymers, hairy-rod polymers tend to self-organize and form microphase-separated structures. For long enough side chains one enters the regime of self-organization, where the tail part of the side chains and the backbones microphase-separate [5,1,6,7,3,8]. A literature survey showed that experimentally, usually involving side chains of a length in the order of 10–15 carbon-carbon bonds, the self-organization observed is mainly in the form of lamellar structures. In order to explain this, we recently presented a theoretical analysis of structure formation in melts of hairy-rod polymers [9]. We showed that three different microphases are possible: one lamellar and two hexagonal. If the side chains are long enough for the elastic stretching free energy of the side chains to completely dominate the repulsive interaction between the backbone and the side chains, hexagonally ordered domains of hairy-rod cylindrical brushes are formed. The lamellar state is found to be stable for shorter side chains and occupies an important part of the phase diagram. In the intermediate side chain length regime a hexagonally ordered structure appears characterized by cylindrical micelles with an elongated core cross-section and containing several hairy-rod polymers.

Self-organization is an example of how nanoscale structures can be formed if different repulsive chemical groups are chemically connected to the same molecules as in the case of the hairy-rod comb copolymers. By contrast, in supramolecular chemistry linking occurs via functional groups that are mutually connected by molecularly matching physical interactions, such as hydrogen bonding, π-stacking, charge transfer, steric match, interpenetrating ring-like structures, etc. [10,11]. Using molecular recognition highly specific complexes called supramolecules can be built, which, in turn, are able to form a hierarchy of structures. Self-organization and supramolecular concepts can naturally be combined to allow structuring [12–15].

[a] e-mail: G.ten.brinke@chem.rug.nl

The possibility of obtaining comb copolymer structures via the supramolecular route, using physical matching interactions, such as ionic, coordination or hydrogen bonding, has attracted a lot of attention lately. Most systems studied involve flexible polymers. However, since the synthesis is so simple, *i.e.* common precipitation in water for polyelectrolyte-surfactant complexes [16,17,13] or solvent casting from a common solvent in the case of hydrogen bonding [18], the natural question arises whether hairy-rod polymers can be prepared via a similar supramolecular route, *i.e.* can hairy-rod molecules be synthesized by simply connecting side chains by "recognizing" driven physical bonds? In the case of rigid-rod polymers, the drastically reduced solubility is a most complicating factor. Still a characteristic example, where this concept works, has been constructed recently involving the rodlike poly(2,5-pyridinediyl) (PPY) [19]. This study demonstrates that it is possible to form processable supramolecular hairy-rod polymer systems. Furthermore, the self-organization due to microphase separation between the backbone and the side chains (of moderate length) has been found to be in the form of a layered structure. In some cases macrophase separation was observed as well. It is the objective of this work to address the phase equilibrium properties of mixtures of rodlike polymers and coil-like chain molecules that are capable of forming hairy-rod supramolecules where the flexible side chains are attached by thermoreversible bonds to the stiff backbone.

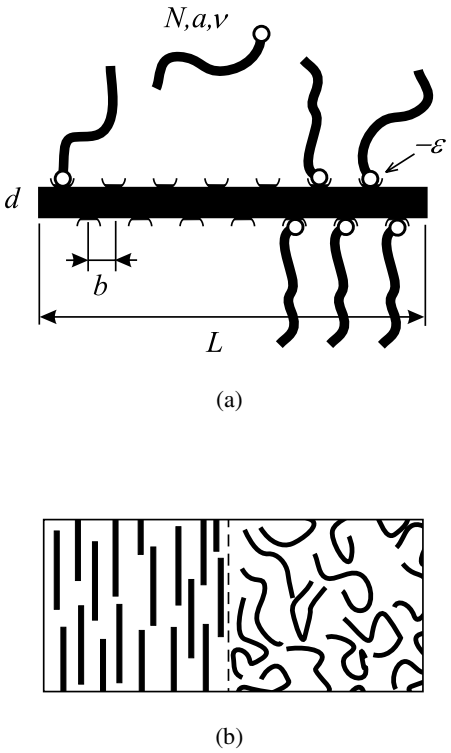

Fig. 1. (a) Model of the hairy rod as a stiff backbone with reversibly attached flexible side chains. (b) Flat interface between pure nematic and isotropic phase.

2 The model

We consider a melt consisting of rigid rods of length L and diameter d ($L \gg d$) and flexible coils consisting of N beads of volume ν and statistical segment length a. The ideal coil size is $R_c = a\sqrt{N}$, $L \gg R_c$. We will assume that each rod contains M associating groups (the average distance between two successive groups is $b = L/M$) which can form bonds with the associating end of the coil (Fig. 1(a)). It is assumed that each coil has only one associating end. The energy of association between rod and coil equals $-\epsilon$. The concentration of rods in the melt is c and their volume fraction is $f = (\pi/4)Ld^2c$.

The interaction between rods and coils can be introduced in the following way [9]. It is well known that rods and polymer coils in the molten state are practically incompatible and separate into a nematic phase consisting of rods and an isotropic phase consisting of the flexible polymer [20,21]. The interface between the nematic and isotropic phase (Fig. 1(b)), is assumed to be sharp and the interfacial tension γ corresponding to the planar orientation of rods at the interface is given by

$$\gamma = (w + sT)/d^2\,, \tag{1}$$

where w is the energetic part of the surface energy and $s > 0$ is the entropic part (here T is temperature in energetic units). According to the definition (1), if a rod penetrates into the polymer melt its free energy loss is approximately equal to

$$\mu_r \simeq 2Ld\gamma\,. \tag{2}$$

Therefore, the free energy of the isotropic phase with a small amount of rigid rods is given by

$$\mathcal{F}_I^* = TVc\ln\left(\frac{f}{e}\right) + TV\frac{1-f}{N\nu}\ln\left(\frac{1-f}{e}\right) + Vc\,\mu_r\,. \tag{3}$$

Here we omitted the interaction between the rods. V is the volume of the system. In (3) the first two terms represent the translational entropy of the rods and coils.

The coils can also penetrate into the nematic phase. In order to write the free energy of the nematic phase with a small amount of coils we introduce the chemical potential of the coil in the nematic phase μ_c which includes both energetic and entropic contributions. Further on we consider the limit

$$\mu_c/T \to \infty \tag{4}$$

for arbitrary T. This means that the coils practically do not penetrate into the nematic phase.

Excluded-volume interaction in the rod-rich phase results in almost perfect alignment of the rods. The free energy of the nematic phase contains also a term connected with orientational ordering of rods. It can be estimated [22,23] as $T\ln(4\pi/\Omega)$, where Ω is the characteristic fluctuation angle, $\Omega \simeq 2\pi(d/L)^2$. Thus, the free energy is

given by

$$\mathcal{F}^*_{\rm N} = TVc\ln\left(\frac{f}{e}\right) + TV\frac{1-f}{N\nu}\ln\left(\frac{1-f}{e}\right) + 2TVc\ln\left(\frac{L}{d}\right) + V\frac{1-f}{N\nu}\mu_{\rm c}\,. \quad (5)$$

The equilibrium between the nematic and isotropic phase can be found in the usual way by equating the chemical potentials and osmotic pressures in both phases:

$$\mu^*_{\rm I} = \mu^*_{\rm N}, \quad \mu^*_{\rm I,N} = \frac{1}{V}\frac{\partial \mathcal{F}^*_{\rm I,N}}{\partial c}\,;$$
$$P^*_{\rm I} = P^*_{\rm N}, \quad P^*_{\rm I,N} = \frac{1}{V}\left(c\frac{\partial \mathcal{F}^*_{\rm I,N}}{\partial c} - \mathcal{F}^*_{\rm I,N}\right)\,. \quad (6)$$

The solution of these equations is given by

$$f_{\rm N} \simeq 1 - \kappa N\exp(-\mu_{\rm c}/T) \simeq 1\,,$$
$$f_{\rm I} \simeq \left(\frac{L}{d}\right)^2 \exp\left(-\frac{2L}{d}\left(\frac{w}{T}+s\right)\right) \ll 1\,. \quad (7)$$

This simple phenomenological model reflects the generic feature of the rod-coil mixtures to phase-separate into almost pure components [24,25]. The corresponding phase diagram is shown in Figure 2(a).

3 Nematic-isotropic liquid phase coexistence: effect of association

In this section we study the influence of association between rods and coils on the macrophase separation described above. We start from the free energy of association between rods and coils, $\mathcal{F}_{\rm bond}$, assuming that they are ideal (without excluded volume). Let p denote the probability that an associating group of the rod has formed a bond with a flexible coil. The total number of bonds in the system is $VMcp$ and equals the number of *associated* coils. Therefore, the number of *free* coils in the system is $(V/N\nu)(1-f-f\kappa pN)$, where $\kappa \equiv \nu/(\pi bd^2/4)$. The free energy of bonds can be expressed through the partition function $Z_{\rm bond}$ as [26–29]

$$\mathcal{F}_{\rm bond} = -T\ln Z_{\rm bond}\,, \quad (8)$$

where

$$Z_{\rm bond} = P_{\rm comb}\left(\frac{v_{\rm b}}{V}\right)^{VMcp}\exp\left(\frac{\epsilon VMcp}{T}\right) \quad (9)$$

and $P_{\rm comb}$ is the number of different ways to link rods and coils for a fixed probability p; $v_{\rm b}$ is the bond volume. If we denote the number of rods in the system as $\mathcal{N}_{\rm r} = Vc$, and the number of coils as $\mathcal{N}_{\rm c} = V(1-f)/N\nu$, then the number of ways to choose $\mathcal{N}_{\rm r}Mp$ coils for bond formation is the binomial coefficient

$$C^{\mathcal{N}_{\rm r}Mp}_{\mathcal{N}_{\rm c}} = \frac{\mathcal{N}_{\rm c}!}{(\mathcal{N}_{\rm r}Mp)!(\mathcal{N}_{\rm c}-\mathcal{N}_{\rm r}Mp)!}\,. \quad (10)$$

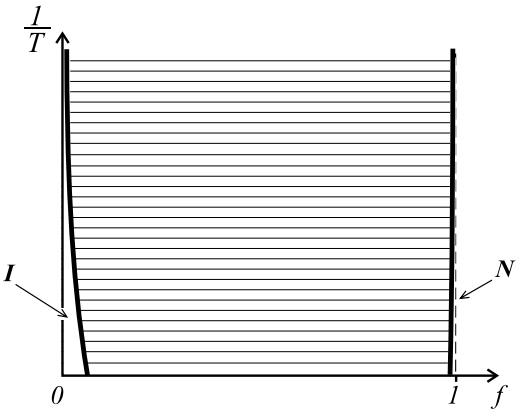

(a)

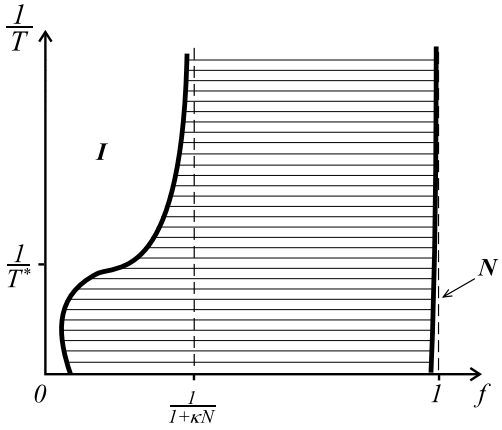

(b)

Fig. 2. Macrophase equilibria in the associating rod-coil system: (a) no compatibility for small association energy; (b) enhanced compatibility in the $\epsilon/w > 2b/d$ case.

Moreover, there are

$$\frac{(\mathcal{N}_{\rm r}M)!}{(\mathcal{N}_{\rm r}M(1-p))!} \quad (11)$$

different ways to select $\mathcal{N}_{\rm r}Mp$ bonds from $\mathcal{N}_{\rm r}M$ associating groups. Therefore,

$$P_{\rm comb} = C^{\mathcal{N}_{\rm r}Mp}_{\mathcal{N}_{\rm c}}\frac{(\mathcal{N}_{\rm r}M)!}{(\mathcal{N}_{\rm r}M(1-p))!} \quad (12)$$

and the free energy of bonds is given by

$$\mathcal{F}_{\rm bond} = VMcp\left[T\ln\left(\frac{N\nu}{v_{\rm b}}\right) - \epsilon\right] + TVcM\left[p\ln p + (1-p)\ln(1-p)\right] + TV\frac{(1-f-f\kappa Np)}{N\nu}\ln\left(\frac{1-f-f\kappa Np}{e}\right) - TV\frac{(1-f)}{N\nu}\ln\left(\frac{1-f}{e}\right)\,. \quad (13)$$

The free energy of the isotropic phase can be written as

$$\mathcal{F}_{\rm I} = \mathcal{F}_{\rm I}^{*} + \mathcal{F}_{\rm bond} + \mathcal{F}_{\rm el}\,, \tag{14}$$

where $\mathcal{F}_{\rm el}$ is the elastic free energy of the side chains of the hairy rod, which appears as soon as the density of association is high enough. We approximate it by [30,31]

$$\mathcal{F}_{\rm el} = \begin{cases} TVc\frac{3\kappa d^2}{32a^2}Mp^2\ln(\kappa Np)\,, & p > \frac{1}{\kappa N}\,, \\ 0, & \text{otherwise}\,. \end{cases} \tag{15}$$

Hence, the final expression for the free energy of the isotropic phase is given by (per volume of one rod $(\pi/4)Ld^2$)

$$\begin{aligned}\frac{F_{\rm I}(f,p)}{T} &= f\frac{\mu_{\rm r}}{T} + Mfp\left[\ln\left(\frac{N\nu}{v_{\rm b}}\right) - \frac{\epsilon}{T}\right] \\ &+fM\left[p\ln p + (1-p)\ln(1-p)\right] + f\ln\left(\frac{f}{e}\right) \\ &+M\frac{(1-f-f\kappa Np)}{N\kappa}\ln\left(\frac{1-f-f\kappa Np}{e}\right) \\ &+f\frac{3\kappa d^2}{32a^2}Mp^2\ln(\kappa Np)\,H\left(p-\frac{1}{\kappa N}\right)\,, \end{aligned} \tag{16}$$

where

$$H(x) = \begin{cases} 1, & x \geq 0\,, \\ 0, & x < 0 \end{cases}$$

is the Heavyside function. Similarly, the free energy of the nematic phase is

$$\begin{aligned}\frac{F_{\rm N}(f,p)}{T} &= 2f\ln\left(\frac{L}{d}\right) + M\frac{1-f}{N\kappa}\frac{\mu_{\rm c}}{T} \\ &+Mfp\left[\ln\left(\frac{N\nu}{v_{\rm b}}\right) - \frac{\epsilon}{T}\right] \\ &+fM\left[p\ln p + (1-p)\ln(1-p)\right] + f\ln\left(\frac{f}{e}\right) \\ &+M\frac{(1-f-f\kappa Np)}{N\kappa}\ln\left(\frac{1-f-f\kappa Np}{e}\right)\,. \end{aligned} \tag{17}$$

The probability of bonding in both phases can be found from the minimization of the corresponding free energies,

$$\frac{\partial F_{\rm I}}{\partial p} = 0, \qquad \frac{\partial F_{\rm N}}{\partial p} = 0 \tag{18}$$

and reads ($N^{*} \equiv N\nu/v_{\rm b}$)

$$\begin{aligned}p = \frac{1}{2\kappa Nf}\Bigg[&1 - f + \kappa Nf - N^{*}e^{-\epsilon/T} \\ &-\sqrt{\left(1-f+\kappa Nf - N^{*}e^{-\epsilon/T}\right)^2 - 4\kappa Nf(1-f)}\ \Bigg] \end{aligned} \tag{19}$$

for the nematic phase and for the isotropic phase when $p < 1/\kappa N$. For $p > 1/\kappa N$, the probability of bonding in the isotropic phase satisfies

$$\ln\left[\frac{pN^{*}e^{-\epsilon/T}}{(1-p)\left(1-f_{\rm I}-f_{\rm I}\kappa Np\right)}\right] + \frac{3\kappa d^2 p}{16a^2}\ln(\kappa Npe) = 0\,. \tag{20}$$

For a small volume fraction of rods, $f_{\rm I} \ll 1$, it is approximately given by

$$\begin{aligned}p &\simeq \frac{1}{1+N^{*}e^{-\epsilon^{*}/T}}, \\ \epsilon^{*} &= \epsilon - \frac{3\kappa d^2 T}{32a^2}\,\frac{1}{1+N^{*}e^{-\epsilon/T}}\ln\left(\frac{\kappa N}{1+N^{*}e^{-\epsilon/T}}\right)\,. \end{aligned} \tag{21}$$

Phase equilibrium between the isotropic and nematic phase can be obtained in a standard way from the equilibrium equations

$$\frac{\partial F_{\rm I}}{\partial f_{\rm I}} = \frac{\partial F_{\rm N}}{\partial f_{\rm N}}\,, \qquad f_{\rm I}\frac{\partial F_{\rm I}}{\partial f_{\rm I}} - F_{\rm I} = f_{\rm N}\frac{\partial F_{\rm N}}{\partial f_{\rm N}} - F_{\rm N}\,, \tag{22}$$

using equations (16,17) together with (19) and (21).

At this point we have to consider two possible situations. The first one occurs if $\kappa N > 1$ so that both $p_{\rm I} < 1/\kappa N$ and $p_{\rm I} > 1/\kappa N$ are possible. The second one corresponds to $\kappa N < 1$, where the elastic tension of the associated coils is not important for any p.

Let us start from $\kappa N > 1$. When the probability of bonding in the isotropic phase $p_{\rm I} < 1/\kappa N$, or equivalently $\epsilon/T < \ln((\kappa N-1)/N^{*})$, expression (19) can be used giving the volume fraction of rods:

$$\begin{aligned}&f_{\rm N} \simeq 1\,, \\ &f_{\rm I} \simeq \left(\frac{L}{d}\right)^2 \exp\left(-\frac{\mu_{\rm r}}{T} + \frac{M}{1+N^{*}e^{-\epsilon/T}}\left(\frac{\epsilon}{T} - \ln N^{*}\right)\right) \ll 1. \end{aligned} \tag{23}$$

However, for lower temperatures $p_{\rm I}$ exceeds $1/\kappa N$ implying that the rods are densely grafted. Then the volume fraction of rods in the isotropic phase $f_{\rm I}$ satisfies the equation

$$\begin{aligned}&\ln f_{\rm I} - Mp_{\rm I}\ln\left(1 - f_{\rm I} - f_{\rm I}\kappa Np_{\rm I}\right) \simeq 2\ln\left(\frac{L}{d}\right) + \frac{M}{N\kappa} \\ &-Mp_{\rm I}\ln N^{*} - \frac{3\kappa d^2}{32a^2}Mp_{\rm I}^2\ln(\kappa N) - \frac{2Ld\gamma}{T} + \frac{Mp_{\rm I}\epsilon}{T}\,, \end{aligned} \tag{24}$$

where $p_{\rm I}$ has to be determined from (20). Obviously, $p_{\rm I} \to 1$ if $T \to 0$ and therefore the last term in (24) becomes dominant. Depending on its sign two characteristic asymptotics can be distinguished:

$$\begin{aligned}f_{\rm I} &\to 0 \qquad \text{if} \quad \epsilon < \frac{2bw}{d}\,, \\ f_{\rm I} &\to \frac{1}{1+N\kappa} \qquad \text{if} \quad \epsilon > \frac{2bw}{d}\,. \end{aligned} \tag{25}$$

Thus, for $\epsilon/w > 2b/d$ rods and coils become partially compatible. This fact has a clear physical meaning. A negative sign of $-\epsilon + (2bw/d)$ corresponds to a negative "total" energy (ϵ-part plus γ-part) due to the association of a coil to a rod, *i.e.* making it favorable to keep *all* coils bonded (for $T \to 0$, of course). In this case (24) gives the fraction of rods in the coil-rich phase and the region of the phase diagram below the temperature

$$T^{*} \simeq \frac{\epsilon - \frac{2bw}{d}}{\frac{2bs}{d} + \ln N^{*} + \frac{3\kappa d^2}{32a^2}\ln(\kappa N)} \tag{26}$$

reveals compatibility enhancement with the asymptotic value of the rod fraction $f_{\mathrm{I}} \to 1/(1+\kappa N)$ for $T \to 0$. This situation is depicted in Figure 2(b): a compatibility region occurs at low temperatures to the left of the stoichiometric point. For small association energies $\epsilon/w < 2b/d$ the situation is qualitatively identical to the one without association (see Fig. 2(a)).

Now we turn to the case $\kappa N < 1$, when only low grafting densities are possible: p_{I} is always less than $1/\kappa N$. So the term responsible for the elastic stretching should be omitted according to approximation (16). This yields an equation for the isotropic phase density analogous to (24) but without the elastic $3\kappa d^2 \ln(\kappa N)/32a^2$ term. In the same way as above, the low-temperature asymptotic $f_{\mathrm{I}} \to 0$ appears for small association energy values corresponding to Figure 2(a). In the opposite case of high energies $\epsilon > 2bw/d$, (24) shows the tendency of f_{I} to increase approaching stoichiometric conditions $1/(1+\kappa N)$. However, it cannot be used in a quantitative manner because it is valid only for an isotropic phase with *small* amount of immersed rods (note that for $\kappa N < 1$ the value of $1/(1+\kappa N)$ is not small anymore).

4 Phase equilibria between nematic, isotropic liquid and microphases for κN > 1

As shown above, the association gives rise to a partial compatibility in the region of volume fractions up to the stoichiometric point $1/(1+\kappa N)$. The existence of this region was proved above under the assumption that the phase is isotropic. However, due to attraction between hairy rods immersed in a flexible-chain melt, the formation of microdomain-ordered structures may be expected.

In general, there are two mechanisms for attraction in hairy-rod systems. The first one arises from the inhomogeneous distribution of the free polymer coils [32] which creates some additional loss of entropy of the coils compared to the homogeneous melt [33]. This mechanism ultimately results in the formation of microdomain lattice structures in the blend.

The second mechanism is connected to the incompatibility of rods and coils and is responsible for the selection between hexagonal and lamellar structures for certain values of the parameters. Furthermore, as in the case of the covalently bonded hairy rods (see Ref. [9]), we can distinguish two different hexagonal phases. In the first one, called H1, the "cylinders" contain only one rod per unit cell ($Q = 1$), Figure 3(a). In the second one, called H2, the surface term becomes more important so that rods attract each other and the cylinders contain $Q > 1$ rods per unit cell, Figure 3(b). On decreasing the temperature the cylinders transform to the lamellar phase.

Additionally, we will prove that the tetragonal phase is unstable and is always suppressed by the hexagonal one.

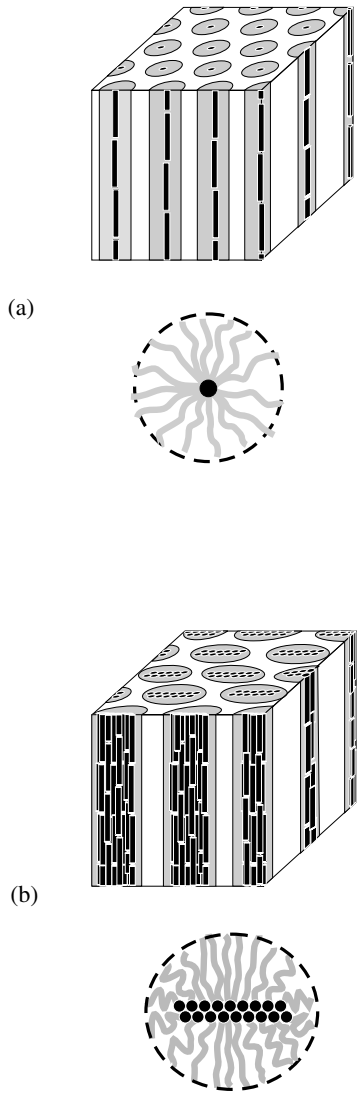

Fig. 3. Possible hexagonal phases: (a) H1; (b) H2.

4.1 Separation of the hexagonal phase H1

The attraction energy of cylinders resulting in the lattice formation of the hexagonal phases (H1, H2) is mainly due to the inhomogeneous distribution of the free polymer coils. Using the random phase approximation, it can be expressed in terms of the fluctuations of the monomeric density in the polymer matrix as [33,32]

$$\frac{\Delta\mathcal{F}}{T} = \frac{N\nu}{2} \int \frac{|\Delta\phi_{\mathrm{free}}(\mathbf{k})|^2}{g\left(\frac{a^2 N\mathbf{k}^2}{6}\right)} \frac{\mathrm{d}\mathbf{k}}{(2\pi)^3}\,. \tag{27}$$

Here $\Delta\mathcal{F}$ is the free-energy change relative to the homogeneous state and $g(u) = 2\left(u - 1 + e^{-u}\right)/u^2$ is the Debye scattering function. $\Delta\phi_{\mathrm{free}}(\mathbf{k})$ denotes the Fourier transform of the function $\phi_{\mathrm{free}}(\mathbf{r}) - 1 \simeq -\phi_{\mathrm{assoc}}(\mathbf{r})$, where ϕ_{free} and ϕ_{assoc} are the volume fractions of the free and associated coils defined at the mesoscopic level. Assuming that all coils obey Gaussian statistics and adopting the superposition approximation [32], where the overall density of

the associated coils $\phi_{\rm assoc}$ is a simple sum of corona's densities of the individual cylinders fixed in the vertices of the lattice, we arrive at the interaction energy (per cylinder of unit length)

$$\frac{\mathcal{U}_{\rm H}(Q)}{T} = \frac{N\nu(Qp)^2}{2b^2}\left[\frac{2}{\sqrt{3}\,\ell^2}\sum_{\{\mathbf{b}_{\rm r}\}}\frac{h^2(\frac{a^2N\mathbf{k}^2}{6})}{g(\frac{a^2N\mathbf{k}^2}{6})} - \frac{1}{4\pi^2}\int \mathrm{d}\mathbf{k}\frac{h^2(\frac{a^2N\mathbf{k}^2}{6})}{g(\frac{a^2N\mathbf{k}^2}{6})}\right], \quad (28)$$

where ℓ is the period of the structure, $\{\mathbf{b}_{\rm r}\}$ are the vectors of the reciprocal lattice, and $h(u) = (1-e^{-u})/u$.

The first term in (28) arises directly from (27), whereas the second one is the energy of the lattice with infinite period, which is used as a reference point. The period of the structure can be easily related to the volume fraction of rods as

$$\ell^2 = \frac{1}{2\sqrt{3}}\,\frac{\pi d^2 Q}{f}\,. \quad (29)$$

After calculation of the sum and integral in (28), we find the interaction energy and renormalize it per volume $(\pi/4)Ld^2$,

$$\frac{U_{\rm H}(Q)}{T} = -\frac{3}{32}\frac{\kappa MQp^2fd^2}{a^2}\left[3.457 + \ln\left(\frac{a^2Nf}{Qd^2}\right)\right]. \quad (30)$$

Thus, the free energy of the H1 phase ($Q=1$) is given by

$$\begin{aligned}\frac{F_{\rm H1}}{T} &= 2fLd\frac{\gamma}{T} - Mfp\left[\frac{\epsilon}{T} - \ln N^*\right] \\ &+ fM\left[p\ln p + (1-p)\ln(1-p)\right] + 2f\ln\left(\frac{L}{d}\right) \\ &+ M\frac{(1-f-f\kappa Np)}{N\kappa}\ln\left(\frac{1-f-f\kappa Np}{e}\right) \\ &+ f\frac{3\kappa d^2}{32a^2}Mp^2\ln(\kappa Np) \\ &- \frac{3}{32}\frac{\kappa Mp^2fd^2}{a^2}\left[3.457 + \ln\left(\frac{a^2Nf}{d^2}\right)\right]. \end{aligned} \quad (31)$$

Here, we approximated the loss of orientational energy of a rod by the term $2Tf\ln(L/d)$ and omitted the loss of its translational entropy because it is relatively small. Phase equilibrium between the isotropic phase and the H1 phase can be found from the equilibrium equations

$$\frac{\partial F_{\rm I}}{\partial f_{\rm I}} = \frac{\partial F_{\rm H1}}{\partial f_{\rm H1}}, \quad \frac{\partial F_{\rm I}}{\partial p_{\rm I}} = \frac{\partial F_{\rm H1}}{\partial p_{\rm H1}} = 0\,,$$

$$f_{\rm I}\frac{\partial F_{\rm I}}{\partial f_{\rm I}} - F_{\rm I} = f_{\rm H1}\frac{\partial F_{\rm H1}}{\partial f_{\rm H1}} - F_{\rm H1}\,. \quad (32)$$

The probability of bonding and the binodal lines are

$$\begin{aligned} &p_{\rm I} \simeq p_{\rm H1} \simeq 1\,, \\ &f_{\rm H1}^{(1)} \simeq \frac{3}{16}\frac{d^2}{a^2N}\,, \\ &f_{\rm I} \simeq \left(\frac{L}{d}\right)^2\exp\left(-\frac{3}{16}\,\frac{d^2\kappa M}{a^2}\right) \simeq 0\,. \end{aligned} \quad (33)$$

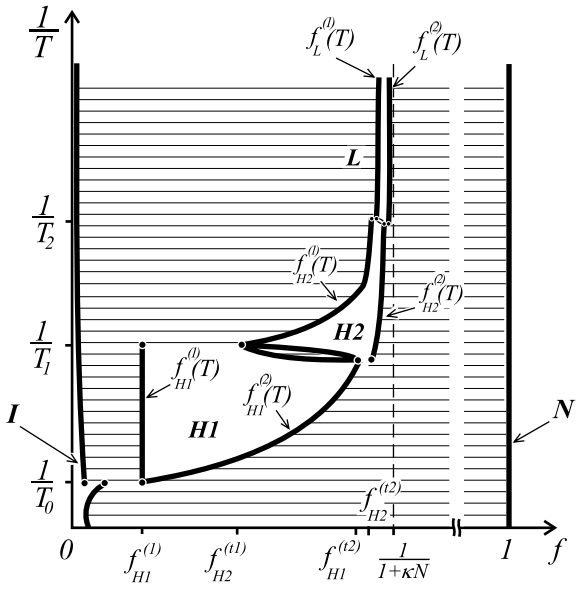

Fig. 4. Complete phase diagram in the case $\kappa N > 1$.

Similarly, the phase equilibrium between the nematic and the H1 phase follows from equations

$$\frac{\partial F_{\rm N}}{\partial f_{\rm N}} = \frac{\partial F_{\rm H1}}{\partial f_{\rm H1}}, \quad \frac{\partial F_{\rm N}}{\partial p_{\rm N}} = \frac{\partial F_{\rm H1}}{\partial p_{\rm H1}} = 0\,,$$

$$f_{\rm N}\frac{\partial F_{\rm N}}{\partial f_{\rm N}} - F_{\rm N} = f_{\rm H1}\frac{\partial F_{\rm H1}}{\partial f_{\rm H1}} - F_{\rm H1}\,. \quad (34)$$

Their solution is given by

$$\begin{aligned} &p_{\rm N} \simeq 0, \quad p_{\rm H1} \simeq 1, \\ &f_{\rm N} \simeq 1, \\ &f_{\rm H1}^{(2)} \simeq \frac{1}{1+\kappa N}\left[1 - \exp\left(-\frac{\epsilon}{T} + 2bd\frac{\gamma}{T} + \ln N^* + \frac{3\kappa d^2}{32a^2}\ln(\kappa N)\right)\right]. \end{aligned} \quad (35)$$

The triple point T_0, where isotropic, nematic and H1 phases coexist, can be obtained from the intersection of the curves $f_{\rm H1}^{(1)}(T)$ and $f_{\rm H1}^{(2)}(T)$ and reads

$$\frac{\epsilon}{T_0} = \frac{1}{1-\frac{2bw}{\epsilon d}}\left(\frac{2bs}{d} + \ln N^* + \frac{3\kappa d^2}{32a^2}\ln(\kappa N)\right), \quad (36)$$

where the probability of bonding $p_0 \simeq 1$. Thus, the hexagonal H1 phase is stable for $f_{\rm H1}^{(1)} < f < f_{\rm H1}^{(2)}$ below T_0; for $f_{\rm I} < f < f_{\rm H1}^{(1)}$ the system separates into the isotropic and the H1 phase and for $f_{\rm H1}^{(1)} < f < f_{\rm N}$ it separates into the H1 and the nematic phase (see Fig. 4).

It is also interesting to note that at the triple point the period of the hexagonal structure is $\ell = \left(8\pi/(3\sqrt{3})\right)^{1/2} a\sqrt{N} \approx 2a\sqrt{N}$ so that the system has the structure of almost close-packed cylinders.

Apparently, a question about the possible existence of a tetragonal (2D square lattice) phase arises at this point. It would correspond to a lower density of rods and might possibly appear at *higher* temperatures $T > T_0$. In the framework of the method employed, the only difference between the H1 and the tetragonal phase is the interaction energy corresponding to the different lattices. The latter is calculated using the same method as explained above (27). It can be shown that the critical point $T_{\rm T}$, at which the tetragonal structure would appear, lies below the point T_0 for any values of the model's parameters: $T_{\rm T} < T_0$. This implies that the tetragonal phase is always suppressed by the hexagonal phase.

4.2 Separation of the hexagonal phase H2

Decreasing the temperature T, we effectively increase the repulsion between the rods and coils due to the surface tension (see, *e.g.*, the first term in (31)). This results in the tendency of rods to adopt a packing with smaller total area of contact with coils. It makes the H2 phase more favorable comparing to the H1, but at the same time leads to an increase in the elastic energy of the side chains (see Fig. 3). The competition between these two factors results in the H1-H2 transition.

Let us follow along the binodal line $f_{\rm H1}^{(1)}(T)$ with the temperature going down (Fig. 4). At a certain moment phase H1 becomes unstable compared to separation into the isotropic and the hexagonal H2 phase. The corresponding triple point can be obtained from the set of equations

$$\frac{\partial F_{\rm I}}{\partial f_{\rm I}} = \frac{\partial F_{\rm H1}}{\partial f_{\rm H1}} = \frac{\partial F_{\rm H2}}{\partial f_{\rm H2}}\,,$$

$$\frac{\partial F_{\rm I}}{\partial p_{\rm I}} = \frac{\partial F_{\rm H1}}{\partial p_{\rm H1}} = \frac{\partial F_{\rm H2}}{\partial p_{\rm H2}} = 0\,, \tag{37}$$

$$f_{\rm I}\frac{\partial F_{\rm I}}{\partial f_{\rm I}} - F_{\rm I} = f_{\rm H1}\frac{\partial F_{\rm H1}}{\partial f_{\rm H1}} - F_{\rm H1} = f_{\rm H2}\frac{\partial F_{\rm H2}}{\partial f_{\rm H2}} - F_{\rm H2}\,.$$

In order to construct the free energy $F_{\rm H2}$ of the H2 phase, one has to modify the surface tension and the elastic-energy terms in (31).

Due to strong incompatibility between rods and coils (see, *e.g.*, (4)) the coils cannot penetrate inside the core of the cylindrical micelle. Therefore, the core adopts a double-layer structure of closely packed rods, as depicted in Figure 3(b), with a surface per unit length along the cylinder $Qd + 2d$ valid for $Q > 2$ (see Ref. [9] for details). For $Q < \sqrt{N}$ the cylinders still have an approximately circular cross-section so that the approximation (15) with renormalized grafting density can be used. Thus,

$$\begin{aligned}\frac{F_{\rm H2}}{T} &= fLd\frac{\gamma}{T}\left(1+\frac{2}{Q}\right) + Mfp\left[\ln N^* - \frac{\epsilon}{T}\right] \\ &+ fM\left[p\ln p + (1-p)\ln(1-p)\right] + 2f\ln\left(\frac{L}{d}\right) \\ &+ M\frac{(1-f-f\kappa Np)}{\kappa N}\ln\left(\frac{1-f-f\kappa Np}{e}\right) \\ &+ f\frac{3d^2\kappa Q}{32a^2}Mp^2\ln(\kappa Np) \\ &- \frac{3}{32}\frac{\kappa MQp^2fd^2}{a^2}\left[3.457 + \ln\left(\frac{a^2Nf}{Qd^2}\right)\right]. \end{aligned} \tag{38}$$

The number of rods per unit cell Q follows from the minimum condition $\partial F_{\rm H2}/\partial Q = 0$,

$$Q \simeq \sqrt{\frac{64ba^2}{3\kappa p^2 d\ln(\kappa N)}\frac{\gamma}{T}}\,. \tag{39}$$

In deriving (39) we used the fact that Q is mainly determined by the interplay between the surface term and the elastic energy of the grafted coils, omitting the relatively small "lattice" term (the last one in (38)).

Hence, the solution of the equations (37) is given by

$$\begin{aligned} &p_{\rm I} \simeq p_{\rm H1} \simeq p_{\rm H2} \simeq 1 \\ &Q_1 \simeq 2+\sqrt{2}, \quad f_{\rm I} \simeq 0, \\ &f_{\rm H1}^{(t1)} \simeq \frac{3}{16}\frac{d^2}{a^2N}, \quad f_{\rm H2}^{(t1)} \simeq \frac{3}{16}\frac{Q_1d^2}{a^2N} \end{aligned} \tag{40}$$

and the critical temperature reads

$$\frac{w}{T_1} \simeq -s + \frac{3\kappa d^3Q_1^2}{64ba^2}\ln(\kappa N) \tag{41}$$

Similarly the binodal line $f_{\rm H2}^{(2)}(T)$ finishes at the triple point, which can be found from the system of equations

$$\frac{\partial F_{\rm N}}{\partial f_{\rm N}} = \frac{\partial F_{\rm H1}}{\partial f_{\rm H1}} = \frac{\partial F_{\rm H2}}{\partial f_{\rm H2}}\,,$$

$$\frac{\partial F_{\rm N}}{\partial p_{\rm N}} = \frac{\partial F_{\rm H1}}{\partial p_{\rm H1}} = \frac{\partial F_{\rm H2}}{\partial p_{\rm H2}} = 0\,, \tag{42}$$

$$f_{\rm N}\frac{\partial F_{\rm N}}{\partial f_{\rm N}} - F_{\rm N} = f_{\rm H1}\frac{\partial F_{\rm H1}}{\partial f_{\rm H1}} - F_{\rm H1} = f_{\rm H2}\frac{\partial F_{\rm H2}}{\partial f_{\rm H2}} - F_{\rm H2}$$

and is characterized by

$$\begin{aligned} &p_{\rm N} \simeq 0, \quad p_{\rm H1} \simeq p_{\rm H2} \simeq 1\,, \\ &Q_1' \simeq Q_1 \simeq 2+\sqrt{2}, \quad f_{\rm N} \simeq 1\,, \\ &f_{\rm H1}^{(t2)} \simeq \frac{1}{1+\kappa N}\left[1 - \exp\left(-\frac{\epsilon}{T_1} + \frac{2bd\gamma}{T_1}\right.\right. \\ &\qquad \left.\left. + \ln N^* + \frac{3d^2\kappa}{32a^2}\ln(\kappa N)\right)\right] \\ &f_{\rm H2}^{(t2)} \simeq \frac{1}{1+\kappa N}\left[1 - \exp\left(-\frac{\epsilon}{T_1} + \frac{bd\gamma}{T_1}\left(1+\frac{2}{Q_1}\right)\right.\right. \\ &\qquad \left.\left. + \ln N^* + \frac{3d^2\kappa Q_1}{32a^2}\ln(\kappa N)\right)\right]. \end{aligned} \tag{43}$$

In a first approximation the corresponding critical temperature coincides with the critical temperature (41). Note the small difference between these critical temperatures, which we do not consider here, results in a small area of phase coexistence between H1 and H2 (see Fig. 4). Also, the triple points $f_{\rm H1}^{(t2)}$ and $f_{\rm H2}^{(t2)}$ are exponentially close to each other. Using (40) and (43), we conclude that the average number of molecules per micelle of length L is $Q_1 = 2 + \sqrt{2} \simeq 3.4$ when H2 first appears. Hence, the cylindrical domain has 3-4 rods in its cross-section. This small number is consistent with the approximation used concerning the almost circular cross-section.

The phase equilibrium between the isotropic and the hexagonal H2 phase is determined from the set of equations

$$\frac{\partial F_{\rm I}}{\partial f_{\rm I}} = \frac{\partial F_{\rm H2}}{\partial f_{\rm H2}}, \quad \frac{\partial F_{\rm I}}{\partial p_{\rm I}} = \frac{\partial F_{\rm H2}}{\partial p_{\rm H2}} = 0\,,$$
$$f_{\rm I}\frac{\partial F_{\rm I}}{\partial f_{\rm I}} - F_{\rm I} = f_{\rm H2}\frac{\partial F_{\rm H2}}{\partial f_{\rm H2}} - F_{\rm H2}\,, \tag{44}$$

which has different asymptotic solutions near the triple point and far away from it. A simple expansion in the vicinity of the $f_{\rm H2}^{(t1)}$ point gives the binodal line in the form

$$f_{\rm H2}^{(1)}(T) \simeq \frac{3}{16}\,\frac{d^2}{a^2 N} Q(T)\,, \tag{45}$$

whereas for $1 \ll Q < \sqrt{N}$ the solution of (44) reads

$$p_{\rm I} \simeq p_{\rm H2} \simeq 1,$$
$$f_{\rm I} \simeq 0,$$
$$f_{\rm H2}^{(1)} \simeq \frac{1}{1+\kappa N}\left[1 - \exp\left(-\frac{3}{16}\frac{d^2}{a^2 N}\,Q(T)\right)\right]. \tag{46}$$

Here $Q(T)$ is given by (39) and is temperature dependent.

Similar equilibrium conditions have to be applied to the nematic-H2 coexistence yielding the result

$$p_{\rm N} \simeq 0, \quad p_{\rm H2} \simeq 1,$$
$$f_{\rm N} \simeq 1,$$
$$f_{\rm H2}^{(2)} \simeq \frac{1}{1+\kappa N}\left[1 - \exp\left(-\frac{\epsilon}{T} + \frac{bd\gamma}{T}\left(1 + \frac{2}{Q(T)}\right)\right.\right.$$
$$\left.\left. + \ln N^* + \frac{3d^2\kappa Q(T)}{32a^2}\ln(\kappa N)\right)\right]. \tag{47}$$

The results obtained for the binodal lines and the triple points are summarized in Figure 4.

With further decrease of the temperature the number of rods in the cross-section Q increases going beyond the limit $Q < \sqrt{N}$. The core of the cylinders containing the rods becomes considerably elongated and the approximation (15) fails. It this case a planar rather than a circular cylindrical shape of the core should be taken as a reference state, reflecting the very high values of $Q \sim N$ in the vicinity of the hexagonal-H2-to-lamellar phase transition. We will address this in the next section.

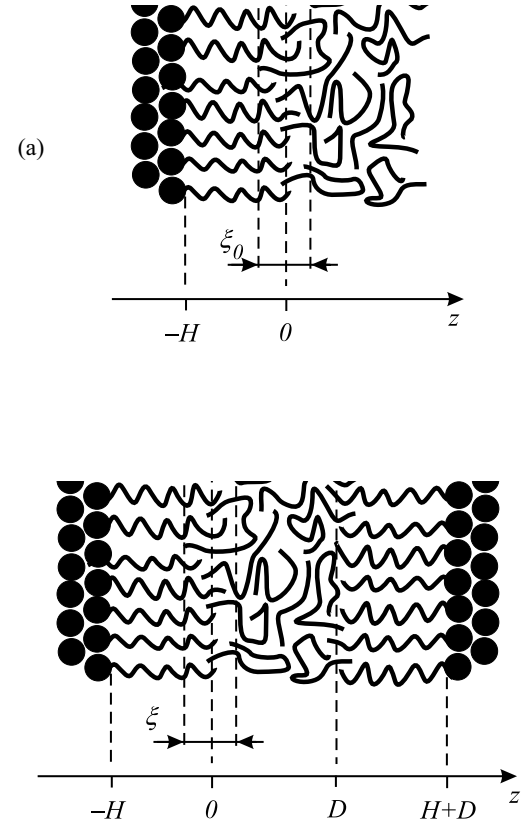

Fig. 5. (a) Single lamella and its surrounding. (b) Two neighboring lamellae.

4.3 Separation of the lamellar phase

Following the same procedure as before, we proceed with the derivation of the free energy of the lamellar phase. Compared to the hexagonal phases, a number of terms has to be modified. Here we start from *the interaction between lamellae*.

Apparently, the total energy of the lamellae's interaction is a sum of all the nearest-neighbor interaction energies. We briefly outline how to calculate this (see Refs. [32, 34] for details). Let us consider first a *single* lamella immersed in a melt of flexible chains. The free-energy per unit area of the lamella consists of the free energy of the attached $\Delta F^{(\rm a)}$ and free $\Delta F^{(\rm f)}$ coils,

$$\Delta F = \Delta F^{(\rm a)} + \Delta F^{(\rm f)}. \tag{48}$$

The last one is given by

$$\Delta F^{(\rm f)} = \frac{a^2 T}{24\nu}\int \frac{(\nabla\phi_{\rm f})^2}{\phi_{\rm f}}{\rm d}z\,.$$

where $\phi_{\rm f}(z)$ is the volume fraction of the free coils and the z-axis points perpendicular to the lamella's plane (see Fig. 5(a)). The $\Delta F^{(\rm a)}$ term consists of two parts,

$$\Delta F^{(\rm a)} = \frac{a^2 T}{24\nu}\int \frac{(\nabla\phi_{\rm a})^2}{\phi_{\rm a}}{\rm d}z$$
$$-\frac{T}{\nu}\int_0^\infty u(z)\left[\phi_{\rm a}(z) - \phi_{\rm a}^{(\rm box)}\right]{\rm d}z\,, \tag{49}$$

where the second term takes into account the additional energy of the attached coils' elastic elongation compared to its minimum value, corresponding to a box-like density distribution $\phi_{\rm a}^{(\rm box)}(z)$. Here

$$u(z) = \frac{3\pi^2}{8}\,\frac{(z+H)^2}{N^2a^2} \tag{50}$$

is the parabolic molecular field responsible for the stretching of the attached coils [34,35] and H is the width of the corona consisting of the attached coils. The deviation from the box-like distribution creates an interpenetration area ξ_0 (see Fig. 5(a)), which in turn is determined from the minimization of (48) with a trial function of the form

$$\phi_{\rm a} = 1 - \phi_{\rm f} = \frac{1}{2}\left(1 - \tanh\frac{z}{\xi_0}\right). \tag{51}$$

After the minimization, ξ_0 is obtained:

$$\xi_0 = \left(\frac{4}{3\pi^4}\,\frac{N^2a^4}{H}\right)^{1/3}, \tag{52}$$

as well as the free energy of the lamella

$$\Delta F_\infty = \min_{\xi_0}\Delta F = \frac{\pi T}{8\nu}\left(\frac{3\pi a^2 H}{4N^2}\right)^{1/3}. \tag{53}$$

Using the same approach, the interaction between two lamellae can be considered too. For this purpose, we examine two planar micelles put on a distance D from each other as depicted in Figure 5(b). Their interaction energy (per unit area) reads

$$\mathcal{U}(D) = \Delta F(D) - 2F_\infty\,, \tag{54}$$

where similarly to the previously explained case

$$\Delta F(D) = \min_{\xi}\left[2\Delta F^{(\rm a)}(\xi) + \Delta F^{(\rm f)}(\xi, D)\right]. \tag{55}$$

Of course, ξ depends now on D; also an appropriate trial function has to be taken for the minimization procedure

$$\phi_{\rm f}(z) = \frac{1}{2}\left[\tanh\frac{z}{\xi} + \tanh\frac{D-z}{\xi}\right]. \tag{56}$$

Without going into details of the calculation, we present the final result (see also Refs. [32,34])

$$\begin{aligned}\xi_{\min}(D) &\simeq \xi + \frac{4}{9}D\,,\\ \xi &= \left(\frac{2}{3\pi^4}\,\frac{N^2a^4}{H}\right)^{1/3}\end{aligned} \tag{57}$$

and

$$\Delta F(D) \simeq \frac{a^2T}{8\nu\xi} + \frac{a^2TD}{18\nu\xi^2}\,. \tag{58}$$

The variables D and H can be easily related to the volume fraction of rods f and other characteristic quantities of the system as

$$\begin{aligned}D &= \frac{\pi d}{2}\,\frac{f^* - f}{{f^*}^2}\,,\\ H &= \frac{\pi d}{4}\kappa N p\,,\end{aligned} \tag{59}$$

where $f^* = 1/(1+\kappa N p)$ is the volume fraction of rods if all coils in the system are attached.

Hence, using equations (54) and (57–59), and renormalizing the energy as per volume $\pi d^2 L/4$, the interaction energy is obtained:

$$\begin{aligned}\frac{U_{\rm L}(f)}{T} &= -0.227 f^* M\left(\frac{pa^2}{\kappa^2 d^2 N}\right)^{1/3}\\ &\quad +1.312 M\left(\frac{p^2d^2}{\kappa a^2 N^2}\right)^{1/3}\frac{f^* - f}{f^*}\,.\end{aligned} \tag{60}$$

The expression for the *elastic free energy* of the coils attached to a planar surface is trivial considering that the stretching free energy of one coil is [36,37] $F_1 = 3TH^2/(2Na^2)$.

So far the free energy of the lamellar phase is obtained in the form

$$\begin{aligned}\frac{F_{\rm L}}{T} &= fLd\frac{\gamma}{T} + Mfp\left[\ln N^* - \frac{\epsilon}{T}\right]\\ &\quad + fM\left[p\ln p + (1-p)\ln(1-p)\right] + 2f\ln\left(\frac{L}{d}\right)\\ &\quad + M\frac{(1 - f - f\kappa N p)}{\kappa N}\ln\left(\frac{H}{\xi}\,\frac{1 - f - f\kappa N p}{e}\right)\\ &\quad + f\frac{3\pi^2 d^2\kappa^2}{32a^2}NMp^3 + \frac{U_{\rm L}(f)}{T}\,,\end{aligned} \tag{61}$$

where ξ, according to (57) and (59), is given by

$$\xi = \frac{2a}{\pi}\left(\frac{aN}{3\pi^2\kappa p d}\right)^{1/3}.$$

Here we have taken into account that any given free coil is confined in a space of width 2ξ between a pair of two successive lamellae separated by a distance $2H$. Therefore, the free coils additionally loose some translational entropy compared to the hexagonal and isotropic phase.

The phase equilibrium between the isotropic and the lamellar phase can be described on the basis of the equations

$$\begin{aligned}&\frac{\partial F_{\rm I}}{\partial f_{\rm I}} = \frac{\partial F_{\rm L}}{\partial f_{\rm L}}, \quad \frac{\partial F_{\rm I}}{\partial p_{\rm I}} = \frac{\partial F_{\rm L}}{\partial p_{\rm L}} = 0\,,\\ &f_{\rm I}\frac{\partial F_{\rm I}}{\partial f_{\rm I}} - F_{\rm I} = f_{\rm L}\frac{\partial F_{\rm L}}{\partial f_{\rm L}} - F_{\rm L}\end{aligned} \tag{62}$$

and the probability of bonding and the binodals are given by

$$\begin{aligned} &p_{\rm I} \simeq p_{\rm L} \simeq 1\,, \\ &f_{\rm I} \simeq 0\,, \\ &f_{\rm L}^{(1)} \simeq \frac{1}{1+\kappa N}\left[1-\frac{\xi}{H}\exp\left(-1.312\left(\frac{\kappa^2 d^2 N}{a^2}\right)^{1/3}\right)\right]. \end{aligned} \tag{63}$$

Similarly, the equilibrium between the nematic and the lamellar phase must fulfill the set of equations

$$\begin{aligned} &\frac{\partial F_{\rm N}}{\partial f_{\rm N}} = \frac{\partial F_{\rm L}}{\partial f_{\rm L}}, \quad \frac{\partial F_{\rm N}}{\partial p_{\rm N}} = \frac{\partial F_{\rm L}}{\partial p_{\rm L}} = 0\,, \\ &f_{\rm N}\frac{\partial F_{\rm N}}{\partial f_{\rm N}} - F_{\rm N} = f_{\rm L}\frac{\partial F_{\rm L}}{\partial f_{\rm L}} - F_{\rm L} \end{aligned} \tag{64}$$

from which the corresponding probabilities and binodals are obtained:

$$\begin{aligned} &p_{\rm N} \simeq 0, \quad p_{\rm L} \simeq 1, \\ &f_{\rm N} \simeq 1, \\ &f_{\rm L}^{(2)} \simeq \frac{1}{1+\kappa N}\left[1-\exp\left(\frac{-\epsilon + bd\gamma}{T}\right.\right. \\ &\qquad \left.\left. + \ln N^* + \frac{3\pi^2 d^2 \kappa^2 N}{32 a^2}\right)\right]. \end{aligned} \tag{65}$$

Now we would like to address the question about the hexagonal-H2-to-lamellar phase transition. As was pointed out before, in the vicinity of the transition the core of the H2 phase cylinders have a considerably non-circular shape (Fig. 3(b)). Therefore, the calculation of the elastic energy and the interaction between this kind of cylinders becomes a nontrivial task. However, taking into account the highly elongated shape of the cores of the H2 cylinders near the transition, the elastic free energy of the side chains can be approximated as that of the corresponding planar lamella plus some edge correction following the method developed in reference [38]. Here we do not go into details of the calculation referring the reader to our recent publication on self-organization of *covalently* bonded hairy-rod system [9], were the following expression has been obtained for this edge correction:

$$\widetilde{F} \simeq -\frac{3fT}{Q}\,\frac{\nu H^2 M p^2}{a^2 b d^2}\,. \tag{66}$$

Hence, the elastic free energy of the H2 phase *near* the H2-to-lamellar phase transition is approximated by

$$\frac{F_{\rm H2}^{\prime\,(\rm el)}}{T} \simeq \frac{3\pi^2 d^2 \kappa}{32 a^2} f N M p^3 - 3\left(\frac{\pi\kappa}{4}\right)^3 \frac{d^2 N^2 M p^4}{a^2}\,\frac{f}{Q}\,. \tag{67}$$

In the very vicinity of the transition between H2 cylinders and lamellae the interaction energy in the H2 phase can be approximated by the corresponding one for the lamella (60), yielding

$$\begin{aligned} \frac{F'_{\rm H2}}{T} &= fLd\frac{\gamma}{T}\left(1+\frac{2}{Q}\right) + Mfp\left[\ln N^* - \frac{\epsilon}{T}\right] \\ &\quad + fM\left[p\ln p + (1-p)\ln(1-p)\right] + 2f\ln\left(\frac{L}{d}\right) \\ &\quad + M\frac{(1-f-f\kappa N p)}{\kappa N}\ln\left(\frac{1-f-f\kappa N p}{e}\right) \\ &\quad + \frac{F_{\rm H2}^{\prime\,(\rm el)}}{T} + \frac{U_{\rm L}}{T}\,. \end{aligned} \tag{68}$$

Comparing (68) to (61), one concludes that the H2-Lam transition is completely determined by the interplay between the elastic and the surface tension term. The quantitative result follows from the equilibrium conditions:

$$\begin{aligned} &\frac{\partial F_{\rm L}}{\partial f_{\rm L}} = \frac{\partial F'_{\rm H2}}{\partial f_{\rm H2}}, \quad \frac{\partial F_{\rm L}}{\partial p_{\rm L}} = \frac{\partial F'_{\rm H2}}{\partial p_{\rm H2}} = 0\,, \\ &f_{\rm N}\frac{\partial F_{\rm L}}{\partial f_{\rm L}} - F_{\rm L} = f_{\rm H2}\frac{\partial F'_{\rm H2}}{\partial f_{\rm H2}} - F'_{\rm H2}. \end{aligned} \tag{69}$$

The area of the lamellar-H2 phase coexistence is very narrow, as it was in the H1-H2 case, implying that the corresponding triple points (H2-Lam-Nem and H2-Lam-Iso; see Fig. 4) are exponentially close to each other and characterized by the temperature T_2,

$$\frac{w}{T_2} \simeq \frac{3}{2}\left(\frac{\pi\kappa d}{4}\right)^3 \frac{N^2}{ba^2} - s\,. \tag{70}$$

Note that the number of rods per cylinder in the H2 phase dropped out from the result (70) *without* minimization. This fact is connected to the approximation (67), which in a sense can be viewed as an expansion in the small parameter $1/Q$. So, to obtain the number of rods Q_2 at the H2-Lam transition consistently one has to extend the approximation (67). However, Q_2 can be also estimated from (67) when the edge correction becomes of the order of the main term

$$Q_2 \sim \kappa N\,. \tag{71}$$

4.4 Possible phase sequences

In the previous sections a complete phase diagram was described for the highly grafted supramolecular hairy-rod system. However, an implicit assumption about the presence of all the three microphases was used. Certainly, depending on the values of the model's parameters (mainly the ratio ϵ/w) other sequences of microphases are possible.

The prediction about the realization of a particular phase diagram can be made from a comparison of the temperatures where the microphases first appear. For instance, the simple hexagonal-phase H1 is present if the temperature T_0 given by (36) is higher than T_1 (41), where a transition to H2 occurs. This leads to the conclusion that the phase diagram has the form shown in Figure 4 only if

$$\frac{\epsilon d}{2bw} > 1 + \frac{\frac{3\kappa d^2}{32a^2}\ln(\kappa N) + \ln N^* + \frac{2bs}{d}}{\frac{3\kappa d^2}{32a^2}(6+4\sqrt{2})\ln(\kappa N) - \frac{2bs}{d}}\,. \tag{72}$$

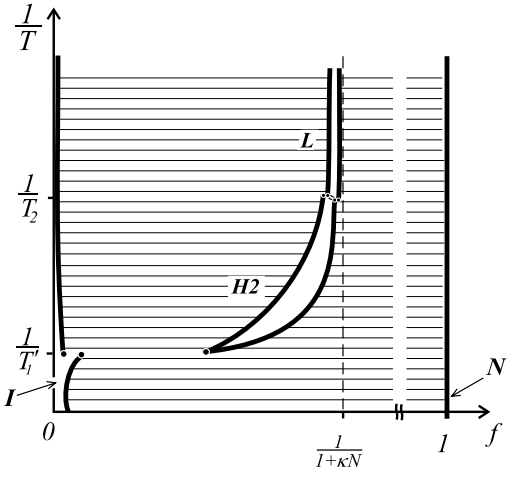

(a)

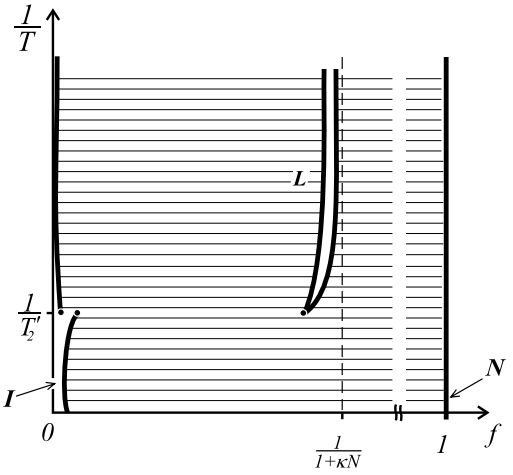

(b)

Fig. 6. Two more possible phase diagrams in the $\kappa N > 1$ (see also Fig. 4 and Eqs. (72, 73)).

In the absence of both hexagonal phases, the lamellar phase would appear at the point determined as the intersection of the curves $f_{\rm L}^{(1)}(T)$ and $f_{\rm L}^{(2)}(T)$ (Eqs. (63, 65)). This point is lower than T_2 (24) if the following condition is fulfilled:

$$1 < \frac{\epsilon d}{bw} < 1 + \frac{4b}{\pi d \kappa N}\,. \qquad (73)$$

Thus, only nematic, isotropic and lamellar phases coexist in this case and the corresponding diagram is shown in Figure 6(b).

Finally, for values of ϵ/w lying in between that of the regimes (72) and (73), only H2 and lamellar structures are stable as depicted in Figure 6(a).

5 Phase equilibria for κN < 1

In this section we consider the phase behavior of the same rod-coil system as before, but for small values of the parameter $\kappa N < 1$. As explained above, this implies a low grafting density of coils attached to a rod even for conversion $p = 1$. A direct consequence in the framework of the presented model is the absence of the elastic stretching term in the free energies of all phases considered. In fact, the free energies of the isotropic liquid and both hexagonal phases can be borrowed from the previous calculation, equations (16, 31, 38), keeping in mind that the term responsible for the stretching of coils has to be omitted everywhere.

However, the lamellar phase needs some additional attention. The expression for the lattice free energy (60) was obtained by a method [32,34] assuming high surface density of the attached coils. Definitely, for $\kappa N < 1$ this is not the case anymore. Therefore, another method, based on (27), should be adopted for this purpose. Using the same arguments as for the hexagonal phase (see (28)) one arrives at the expression for the lattice energy of the lamellar structure:

$$\frac{U_{\rm L}'(f)}{T} \simeq \frac{\pi^2}{128}\,\frac{M\kappa p^2 d^2}{a^2} + \frac{Mf\kappa p^2 d\sqrt{N}}{8a}\left[-1.728 + \frac{af\sqrt{N}}{d}\right]. \qquad (74)$$

Therefore, the total free energy of the lamellar phase (per volume of a rod) reads

$$\frac{F_{\rm L}'}{T} = fLd\frac{\gamma}{T} + Mfp\left[\ln N^* - \frac{\epsilon}{T}\right] + \frac{U_{\rm L}'(f)}{T} + fM\left[p\ln p + (1-p)\ln(1-p)\right] + 2f\ln\left(\frac{L}{d}\right) + M\frac{(1-f-f\kappa Np)}{\kappa N}\ln\left(\frac{H}{\xi}\,\frac{1-f-f\kappa Np}{e}\right). \qquad (75)$$

Further analysis shows that, in contrast to the previously considered high grafting density situation, only the lamellar structure accompanied by nematic and isotropic liquid is present in the phase diagram of Figure 7. It first appears at the temperature

$$\frac{1}{T_2} = \frac{\ln N^* + bs/d}{\epsilon - bw/d} \qquad (76)$$

and takes a prominent place in the phase diagram totally suppressing both hexagonal phases.

This fact is also supported by our physical expectations. The actual selection between H1, H2 and Lam phases in the case $\kappa N > 1$ was performed by an interplay between the surface tension γ-term and the elastic stretching of the side chains. At relatively high temperatures, the surface tension was small and therefore the system adopted the hexagonal structure characterized by lower elastic energy. However, as the temperature is decreased, the surface tension starts to play the dominant role and

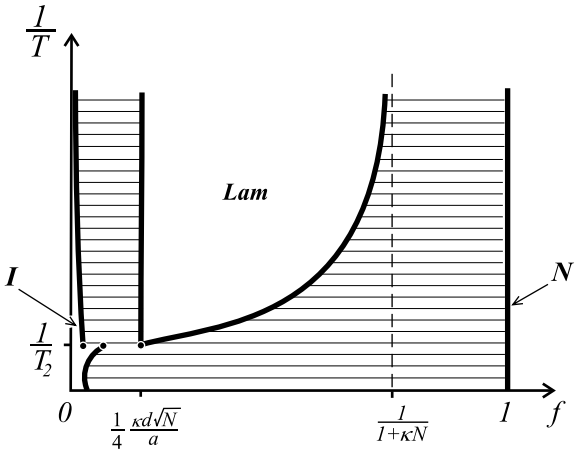

Fig. 7. Phase diagram of the system for $\kappa N < 1$.

the system transforms to the lamellar phase where the total contact area between rods and coils is much smaller. In the current case of $\kappa N < 1$, the elastic energy is not important at all. This implies the dominant position of the lamellar phase (compared to hexagonal) for any value of the model parameters.

Proceeding with the binodal lines we write the standard equilibrium conditions for the isotropic-lamellar coexistence (62) yielding

$$f_{\rm I} \simeq \left(\frac{L}{d}\right)^2 \exp\left(-\frac{Ld\gamma}{T}\right),$$
$$f_{\rm L}^{(1)} \simeq \frac{1}{4}\,\frac{\kappa d\sqrt{N}}{a}. \qquad (77)$$

The same can be done for the equilibrium between the nematic and lamellar phases

$$f_{\rm N} \simeq 1,$$
$$f_{\rm L}^{(2)} \simeq \frac{1}{1+\kappa N}\left[1 - \exp\left(\frac{-\epsilon + bd\gamma}{T} + \ln N^*\right)\right]. \qquad (78)$$

The resulting phase diagram is shown in Figure 7. A large part of it is occupied by the lamellar microphase, which appears above the $1/T_2$-point.

6 Discussion

In this paper we addressed the peculiarities of the phase equilibria and microstructure formation of thermoreversible hairy-rod polymers. The main results are summarized in the phase diagrams of Figures 4, 6 and 7.

We started from a blend of rods and coils, which are in general strongly incompatible, Figure 2(a). It has been shown that thermoreversible association induces a significant compatibility enhancement: for the association energy beyond a certain value, $\epsilon > 2bw/d$, a partial compatibility is achieved at temperatures below T^*, formula (26), to the left from the stoichiometric point (see Fig. 2(b)). The conversion parameter p is close to unity in the coil-rich phase and negligibly small in the rod-rich phase.

Furthermore, the compatibility region was proven to be unstable against microstructure formation. Due to mutual attraction between hairy-rod molecules in a melt of flexible coils, they tend to self-organize. Three types of microphases, namely H1 and H2 hexagonal and lamellar, can appear and coexist with each other as well as with the isotropic and nematic phase (see phase diagrams of Figs. 4, 6 and 7). The actual selection between the different microphases at any given temperature is a result of the competition between the "surface tension" γ-part of the free energy and the elastic stretching of the side chains: the first one is responsible for the tendency of the rods to stick together, whereas the second one, if the hairy-rod is densely grafted, prevents it. This competition leads to the hexagonal H1 phase being stable at relatively high temperatures. For somewhat lower temperatures it is followed by H2 and then by the lamellar microphases (Fig. 4). Actually, depending on the value of the $\epsilon d/bw$ parameter, equations (72) and (73), three different sequences of microphases are possible. For quite small values, see (73), only a narrow strip of the lamellar microphase is present along with the nematic and isotropic phases, Figure 6(b). If $\epsilon d/bw$ is large enough, equation (72), all three microstructures appear, see Figure 4. In the intermediate regime only two phases, H2 and lamellar, are possible. In many respects, this situation resembles that of the covalently bonded system [9], where these three types of sequences were predicted as well.

A qualitatively different situation is observed in the $\kappa N < 1$ case: the grafting density is always low and the elastic part of the free energy is negligibly small. This immediately results in the fact that only the lamellar structure can be found, see Figure 7. Indeed, nothing prevents rods from the γ-driven tendency to keep the contact area with coils as small as possible. The lamellar phase first appears at the triple point T_2, equation (76), and then occupies the lion's share of the diagram (we remind that for $\kappa N < 1$ the stoichiometric point $1/(1+\kappa N) > 1/2$). Existence of the Figure-7–type phase diagram is in accordance with the few experimental data available (Refs. [39–42,19]). In these experimental systems the κN-parameter is definitely less than unity [19]. So, a lamellar structure is expected to be present along with the isotropic and nematic phases (in practice, the latter might correspond to either a nematic or a crystalline phase), which is indeed observed experimentally [40,19].

Authors are grateful to Prof. I. Erukhimovich for helpful remarks. A. Subbotin acknowledges INTAS (grant INTAS-2000-00278) and the Dutch Organization for Scientific Research NWO for financial support.

References

1. M. Ballauff, Angew. Chem., Int. Ed. Engl. **28**, 253 (1989).
2. H. Menzel, in *Polymer Materials Encyclopedia*, edited by J.C. Salamone (CRC Press, Boca Raton, Fla, 1996) p. 2916.
3. G. Wegner, Thin Solid Films **216**, 105 (1992).

4. O. Ikkala, G. ten Brinke, in *Handbook of Advanced Electronic and Photonic Materials and Devices, Part 8, Conducting Polymers*, edited by H.S. Nalwa (Academic Press, San Diego, 2000) Chapt. 5, pp. 185-208.
5. M. Ballauff, Makromol. Chem. **7**, 407 (1986).
6. P. Galda, D. Kistner, A. Martin, M. Ballauff, Macromolecules **26**, 1595 (1993).
7. M. Steuer, M. Hörth, M. Ballauff, J. Polym. Sci. A **31**, 1609 (1993).
8. M. Ballauff, G.F. Schmidt, Makromol. Chem. **8**, 93 (1987).
9. R. Stepanyan *et al.*, Macromolecules **36**, 3758 (2003).
10. J.-M. Lehn, *Supramolecular Chemistry* (VCH, Weinheim, 1995).
11. F. Vögtle, *Supramolecular Chemistry* (Wiley, Chichester, 1993).
12. S.I. Stupp *et al.*, Science **276**, 384 (1997).
13. M. Antonietti, C. Burger, A.F. Thünemann, Trends Polym. Sci. **5**, 262 (1997).
14. G. ten Brinke, O. Ikkala, Trends Polym. Sci. **5**, 213 (1997).
15. J. Ruokolainen *et al.*, Science **280**, 557 (1998).
16. A.F. Thünemann, Prog. Polym. Sci. **14**, 1473 (2002).
17. M. Antonietti, S. Henke, A.F. Thünemann, Adv. Mater. **8**, 41 (1996).
18. O. Ikkala, G. ten Brinke, Science **295**, 2407 (2002).
19. M. Knaapila *et al.*, accepted for publication in J. Phys. Chem. B.
20. P.J. Flory, Macromolecules **11**, 1138 (1978).
21. A. Abe, M. Ballauff, in *Liquid Crystallinity in Polymers*, edited by A. Ciferri (VCH Publishers, New York, 1991) Chapt. 4, pp. 131-167.
22. A.R. Khokhlov, in *Liquid Crystallinity in Polymers*, edited by A. Ciferri (VCH Publishers, New York, 1991) Chapt. 3, pp. 97-129.
23. A.N. Semenov, A.R. Khokhlov, Sov. Usp. Fiz. Nauk **156**, 427 (1988).
24. P.J. Flory, Adv. Polym. Sci. **59**, 1 (1984).
25. M. Ballauff, J. Polym. Sci. B **25**, 739 (1987).
26. A.N. Semenov, M. Rubinstein, Macromolecules **31**, 1373 (1998).
27. I.Y. Erukhimovich, Sov. Phys. JETP **81**, 553 (1995).
28. H.J. Angerman, G. ten Brinke, Macromolecules **32**, 6813 (1999).
29. E. Dormidontova, G. ten Brinke, Macromolecules **31**, 2649 (1998).
30. A. Subbotin, M. Saariaho, O. Ikkala, G. ten Brinke, Macromolecules **33**, 3447 (2000).
31. R. Stepanyan, A. Subbotin, G. ten Brinke, Macromolecules **35**, 5640 (2002).
32. A.N. Semenov, Macromolecules **26**, 2273 (1993).
33. L. Leibler, Macromolecules **13**, 1602 (1980).
34. A.N. Semenov, Macromolecules **25**, 4967 (1992).
35. S.T. Milner, Z.G. Wang, T.A. Witten, Macromolecules **22**, 489 (1989).
36. A.Y. Grosberg, A.R. Khokhlov, *Statistical Physics of Macromolecules* (American Institute of Physics, New York, 1994).
37. P.G. de Gennes, *Scaling Concepts in Polymer Physics* (Cornell University Press, Ithaca, 1985).
38. A.N. Semenov, I.A. Nyrkova, A.R. Khokhlov, Macromolecules **28**, 7491 (1995).
39. M. Knaapila *et al.*, Appl. Phys. Lett. **81**, 1489 (2002).
40. M. Knaapila *et al.*, Synth. Met. **121**, 1257 (2001).
41. H. Kosonen *et al.*, Synth. Met. **121**, 1277 (2001).
42. H. Kosonen *et al.*, Macromolecules **33**, 8671 (2000).